Hybrid additive manufacturing of AISI H13 through InterLayer machining and laser re-melting

BIDARE, Prveen, JIMINEZ, Amaia, ABDELKHALEK, Sherif. M., KHALED, Iman, HASSAN, Ali, ABDALLAH, Ramy and ESSA, Khamis

Published version

BIDARE, Prveen, JIMINEZ, Amaia, ABDELKHALEK, Sherif. M., KHALED, Iman, HASSAN, Ali, ABDALLAH, Ramy and ESSA, Khamis (2023). Hybrid additive manufacturing of AISI H13 through InterLayer machining and laser re-melting. Materials Today Communications, 37: 107042.

HYBRID ADDITIVE MANUFACTURING OF AISI H13 THROUGH INTERLAYER MACHINING AND LASER RE-MELTING

Prveen Bidare [a,b], Amaia Jiménez [c,*], Sherif M. Abdelkhalek [d], Iman Khaled [a], Ali Hassan [e], Ramy Abdallah [a], Khamis Essa[a]

[a] School of Mechanical Engineering, University of Birmingham, Birmingham, UK

[b] Department of Engineering and Mathematics, College of Business, Technology and Engineering, Sheffield Hallam University, Sheffield, S1 1WB, UK

[c] Universidad de Navarra, TECNUN Escuela de Ingeniería, Manuel de Lardizábal 15, 20018, San Sebastián, Spain

[d] Mechanical Design and Production Department, Military Technical College, Cairo, Egypt

[e] School of Computing, Engineering and Digital Technologies, Teesside University, UK.

ABSTRACT

Heat accumulation along the deposited layers in AM is an important issue that may lead to shape distortions. In this context, the present paper is aimed at analysing the feasibility of interlayer post-processing of depositions to improve interlayer bonding and process performance. Concretely, the use of interlayer machining and laser re-melting is tested and their effect on the porosity, mechanical properties and component distortion is analysed. Additionally, the results obtained after each interlayer post-processing technique were compared with an as-deposited sample to analyse the benefits of the hybrid additive manufacturing approach on the generated parts. Samples post-treated through machining showed the lowest deformation. As for the porosity, laser remelting post-processing led to best results. Hardness was also tested along the height of samples and it was observed that it increases in build direction for all the cases tested. Highest hardness values were obtained for the samples post-processed through machining.

Keywords: Hybrid manufacturing; machining; laser re-melting; DLD

1. INTRODUCTION

In the last decades, the manufacturing industry has experienced a huge evolution, especially driven by the appearance of Additive Manufacturing (AM) [1]. Although it was first applied to the manufacturing of plastic prototypes, the development of metal AM technologies has allowed the generation of functional parts through these techniques. Among the different metal additive technologies, Powder Bed Fusion (PBF) and Direct Energy Deposition (DED) are the most commonly employed in the industry [2,3]. Concretely, Laser Powder Bed Fusion (L-PBF) and Direct Laser Deposition (DLD) are the choices that most manufacturers employ for their applications [4], [5]. L-PBF technology allows the generation of complex parts with relatively high accuracy, but part sizes are limited to the size of the powder bed. On the contrary, DLD is a flexible technology that can be integrated into machine centres and allows the generation of a wider range of part sizes with higher productivity [6].

Metal AM provides great benefits regarding design flexibility, reduction of waste material and generation of internal cavities, among others. However, these technologies present also some disadvantages, such as surface roughness, low dimensional accuracy and poor mechanical properties of the generated parts. These issues make them unsuitable for some high-tech applications that require the fulfilment of tough tolerances [7]. In those cases, AM components need to be post-processed to improve their surface finishes, dimensional tolerances and properties. This combination of AM and post-processing is known as Hybrid Additive Manufacturing.

Different post-processing techniques have been shown to enhance the properties and characteristics of AM parts. The beneficial effects of machining and heat treatments on AM parts have been addressed in the literature. According to machining operations, in 2017, the European Group of

Additive Manufacturing [8] presented a comparison between the achievable surface qualities, in terms of surface roughness, in different technologies. According to that work, the roughness of L-PBF parts with no post-processing is between 25-40 μm, while in turning or milling the values decrease to 4 μm and 10 μm, respectively. Similar conclusions about roughness improvement that can be achieved through post-processing machining were presented by Kumbhar et al. [9] in their review paper. Concerning the post-processing through heat treatment, most works reported in the literature focus on solution heat treatment. Special attention has been made to its effect on microstructure and mechanical properties of the treated parts [10], [11]. Tucho et al. [10] post-processed L-PBF parts through solution heat treatment at 1100ºC and 1250ºC for different hold times and observed that stress relief and grain coarsening occurred. Popovich et al. [12] applied different heat treatments along with hot isostatic pressing (HIP) to examine their effect on Inconel 718. The resulting mechanical properties became superior to those of cast and wrought Inconel 718. Hassanin et al. [13] combined L-PBF technology and HIP to produce net-shape components more rapidly and at a lower cost than using L-PBF alone. Ti6Al4V parts were created and a FE model was developed to simulate the deformations of parts as a consequence of the HIP-ing. Geometrical analysis and microstructural characterization were carried out that verified the efficiency of the process.

In addition to solution heat treatment, the so-called laser re-melting (LR) is gaining interest as an alternative for the post-processing of AM parts. LR has shown to decrease the porosity and improve the microstructure of the part. “Laser re-melting” term can be used to refer to scan strategies in which layers have more than one pass of laser scan. The second pass of the laser aimed at generating further material densification, surface quality and microstructural improvement [14]. Recently, Yasa et al. [15] analysed the influence of different process parameters (scan speed, scan spacing and the number of re-melting scans) on the porosity, surface roughness and microhardness of the resulting AISI 316L stainless steel and Ti6Al4V parts. The use of a re-melting scan was observed to improve part characteristics in all cases. Similar conclusions were extracted by Yu et al. [16] that analysed the influence of using different scanning directions for the SLM and the re-melting processes in the roughness and porosities generated. Yang et al. [17] analysed the changes in microhardness and micrographs after re-melting of L-PBF samples. It was shown in their study that laser re-melting refines grains sizes and homogenizes the compositions leading to improvement in hardness of the treated samples. Wei et al. [18] analysed the influence of the number of re-melting scans on the porosity, roughness and residual stress values. It was observed in their study that both the porosity and the roughness decreased no matter the number of scans. However, the residual stresses showed a different trend as they increased in the case of employing one re-melting scan but decreased when two or more re-melting scans were applied.

Concerning the materials employed in AM, this work focuses on AISI H13 chromium-based tool steel, which is widely used in hot and cold work tooling applications due to its high toughness and fatigue resistance [19]. It is used more than any other tool steel in tooling applications and for producing die casting and forging dies [20]. To generate these dies through traditional manufacturing processes such as machining, large blocks of material must be machined and post-process through heat-treatment is usually needed to achieve the full strength of the material. Taking into account the high cost of these processes, AM is a potential alternative to conventional processes as it enables the reduction of machining operations and material waste. Therefore, these processes can drastically reduce the cost of die manufacturing. Some literature works have focused their attention on the use of H13 for AM applications. In 2013, Articek et al. [21] analysed the feasibility of LENS process to create FGM parts based on H13 and Cu. This work aimed to analyse the potential of the technology to create H13-Cu-based FGM components that can enhance the thermal conductivity of H13 tool steel. Telasang et al. [22] analysed the effect of laser parameters on the microstructure and hardness of H13 samples manufactured by laser cladding. Authors employed continuous and pulse-mode laser cladding and conventional and laser-assisted tempering of deposited samples. They observed that 45% higher hardness samples can be achieved by optimizing laser parameters. The hardness of H13 samples generated by AM was also analysed by Park et al. [23]. They observed that in the DLD process, the hardness of H13 samples decreases with the increase of energy input. However, they noted that regardless of the energy input, DLD-ed samples showed higher hardness values than wrought H13. Cottam et al. [20] conducted an experimental study in which wedged samples of H13 were created through direct metal deposition.

Authors analysed residual stresses, microstructure generated and observed that for this wedged geometry, compressive stresses, and high hardness samples were generated that are highly suitable for die manufacturing applications. Recently, Choe et al. [24] conducted a series of experiments in which L-PBF samples of H13 were post-processed through laser re-melting with different scanning speeds. The authors observed that for certain scanning speeds, the porosity of H13 samples can be reduced through re-melting. AM has been also investigated as a suitable solution for H13 die repair. Payne et al. [25] repaired a worn H13 sample through DMD to analyse the suitability of this technology for die repair. Repaired samples were later subjected to high pressure and temperatures to simulate the in-use loading and analyse the behaviour of the re-manufactured components.

Considering the benefits provided by different post-processing techniques to the quality and properties of additively manufactured parts, in this work, the feasibility of interlayer post-processing of additively manufactured samples to improve the interlayer bonding and, in turn, reduce component porosity and distortion and improve mechanical properties is studied. Concretely, machining and laser re-melting have been tested as interlayer post-processing alternatives. Porosity, mechanical properties and distortion of AM samples treated through both techniques have been compared. The number of layers deposited before applying the post-processing treatment has been varied for each sample to analyse the influence of this parameter on the characteristics of generated parts as well. The properties of machined and heat-treated samples are also compared to those of the as-deposited sample to prove the benefits of the hybrid additive manufacturing approach. Additionally, temperatures that rise during the process and for each post-processing method are also studied in order to study any potential correlation between process temperatures and final results.

2. MATERIALS AND METHODS

A gas atomised H13 powder was used to produce test samples on a Mazak Integrex i-400AM hybrid manufacturing machine that combines L-DED additive technology and multi-axis machining operations in a single setup [26]. For the additive process, the Integrex machine employs a 1kW single-mode fibre laser with a 1.064 μm wavelength.

H13 steel alloy that is commonly employed in the tooling industry for production of tools and dies for various manufacturing applications was chosen for the samples. This material selection was due to the high applicability of additive and hybrid additive manufacturing on the repair of tools and dies for this industry. Results from a chemical analysis performed by the powder supplier on the H13 powder used in these tests are shown in Table 1 [27].

Fe	Cr	Mo	Si	V	C
Balance	5%	1%	1%	1%	0.4%

Table 1. Chemical composition of the H13-B powder employed in the tests.

Additional information about powder size distribution and characteristics is included in Figure 1, these tests were conducted in-house to benchmark the powder for this study.

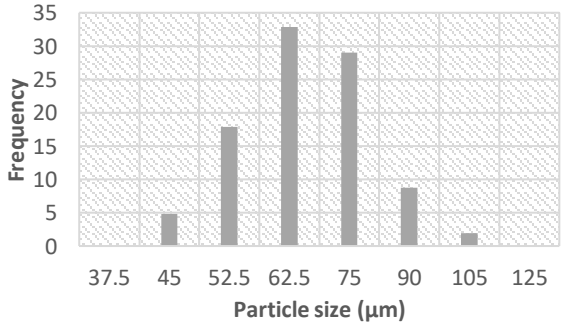

Figure 1. Particle size distribution of the H13 powder employed in the experiments.

In the experiments, wall samples were built through multi-layered single-track deposition on 304 stainless steel substrates. The length of the wall samples was 30 mm, the height was ~15 mm, and the width of the wall was ~2 mm which is equal to single track width. The interlayer machining and laser remelting (LR) operations were conducted on the same machine and using a single setup during the whole manufacturing of each sample. In order to select the optimal process parameters, preliminary tests were conducted first for wide ranges of process parameter values. Based on the results obtained on those tests the parameters that led to best single-track results (summarized in Table 2) were selected for the depositions in the main experiments.

Laser power	Laser travel speed	Spot size	Powder flow rate	Programmed layer thickness
800 W	250 mm/min	2 mm	6 gr/min	0.8 mm

Table 2. DLD process parameters.

Once the most suitable additive process parameters were selected, the main tests were conducted combining L-DED with interlayer machining and interlayer laser re-melting. Figure 2 shows a schematic diagram of both post-processing techniques.

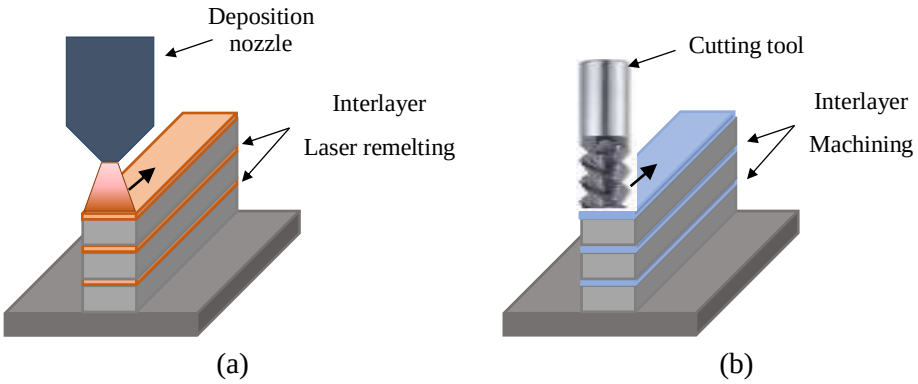

Figure 2. Schematic diagram of post-processing operations: (a) laser re-melting and (b) machining (face-milling).

As mentioned in the introduction, a different number of layers were deposited for each sample before applying the interlayer treatment to analyse how this parameter could influence the final result. Table 3 shows the experimental plan for each sample. Face-milling (Figure 2 (a)) and laser re-melting (Figure 2 (b)) of the top surface of the samples were employed alternatively in different layers of the sample. As it is seen in the table, two samples were created with no interlayer treatment to compare characteristics of as-deposited and interlayer treated samples and verify the improvement provided by each of them. Additionally, the influence of dwell time between consecutive depositions was analysed too. With this aim, one of the samples was built with no dwell time between depositions, whereas in the other, a dwell time of 10 seconds was set between successive scans.

Test no.	Post-processing	Nº of layers between interlayer treatment
1	Only L-DED and no dwell time	-
2	Only L-DED and 10s dwell time	-
3	Machining	Every 2 layers
4		Every 5 layers
5		Every 10 layers
6	Laser re-melting	Every 2 layers
7		Every 5 layers

8	Every 10 layers

Table 3. Summary of experimental tests.

During laser re-melting interlayer treatment, the laser power was reduced to 500W, the standoff distance was extended from 10 mm to 21 mm to provide a larger defocused beam diameter, and the same scanning speed used for depositions (250 mm/min) was employed. In the interlayer treatment through face-milling, cutting conditions suggested by the tool manufacturer for the machining of H13 steel were selected. Concretely, tool rotation speed and feed were set to 5000 rpm and 100 mm/min, respectively. Additionally, a step depth of 0.4 mm was used for machining the upper surface of the given layer in the sample being built.

As it is known, temperature has a great influence on the integrity of the AM components. Therefore, during depositions and interlayer treatment operations, temperatures were measured through an Optris PI 1M thermal imaging camera. The temperature values and concretely, cooling rates have a great effect on the precipitation of different phases, on the resulting microstructure and, in turn, on the obtained component properties. Therefore, this parameter was analysed for different deposition strategies to increase process understanding and to find any possible correlation between temperatures that arise during the process and final results.

In addition to temperature measurements, macro and micro-scale analysis of the samples was also conducted. The possible deformation of as-deposited and post-processed samples with respect to the theoretical model of the walls was measured. The shapes and dimensions of the samples were compared with the intended geometry (CAD model). Samples were then ground and polished before they were cut in the transversal and longitudinal directions to analyse their microstructure and density through Hitachi TM3030 SEM equipment. Finally, the evolution of hardness along the sample height was also analysed for all the samples. An Indentec 5030 SKU equipment was employed to obtain the Vickers hardness through indentation tests following the ASTM E-384 standard with a 500gm load. Hardness values were measured from the top surface of the samples at different depths in steps of 2 mm between each other.

In the following sections, results obtained during the experimental tests will be presented and discussed.

3. RESULTS

In this section, the most relevant results extracted from the experimental work are presented and analysed. Figure 3 shows H13 samples deposited during the experiments that correspond to different interlayer treatment strategies. For each case, the cross-section of the sample that was employed for porosity analysis is also included.

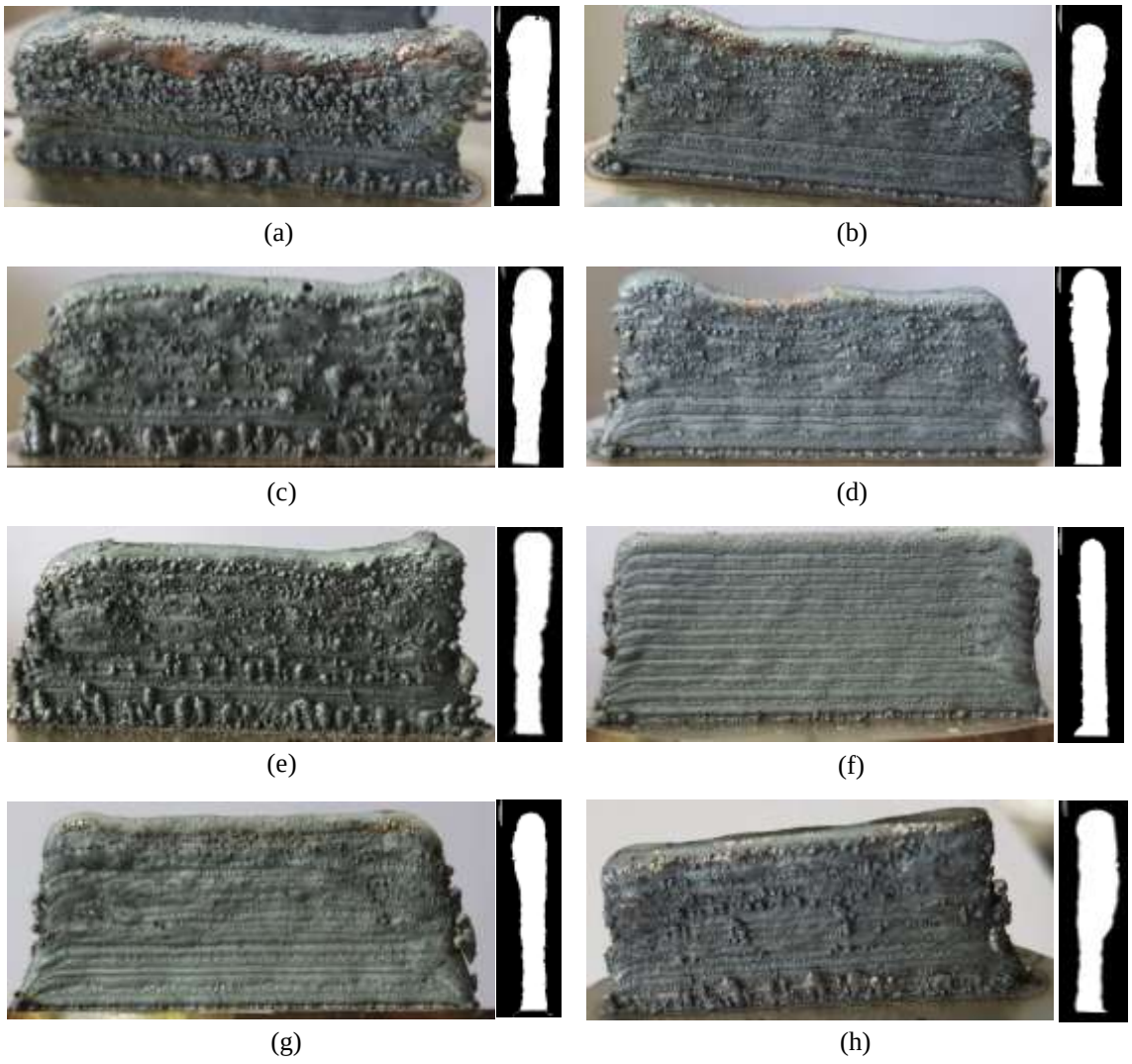

Figure 3. H13 walls deposited with different post-processing strategies: as-deposited with (a) no dwell time and (b) with 10 s dwell time; interlayer post-processing by laser-remelting (c) every two layers, (d) every five layers and (e) every ten layers; and interlayer post-processing through machining (f) every two layers, (g) every five layers and (h) every ten layers.

In Figure 3 (a) an as-deposited H13 wall is shown that was not subjected to any interlayer treatment. It can be seen that the deposition is highly distorted from a theoretical straight wall. Additionally, the upper layers show a great amount of oxidation and powder accumulated on the extremes of the tracks that exacerbate the deformation of successive layers. Figure 3 (b) shows the wall generated with no post-processing, but with a 10 s dwell time between layers. Even if the wall is still highly distorted, it can be seen that during the deposition of the first layers, the applying a dwell time between layers improves process performance and better depositions can be achieved. Figure 3 (c), (d) and (e) show depositions in which interlayer post-processing through LR was applied every two, five and ten deposited layers, respectively. It is seen that generated samples still present a high distortion, similar to the one shown by the as-deposited walls. However, oxidation between layers is apparently reduced. Finally, Figure 3 (f), (g) and (h) show the samples in which interlayer machining was applied every two, five and ten layers, respectively. It is observed that in these cases, the deformation of the wall is minimal compared to the other samples. The depositions are quite uniform and regular and the amount of material accumulated in the extremes of each track is almost negligible compared to the other two cases. In comparing the three samples it is extracted that wall distortion increases with the increase in number of layers deposited before post-processing is applied. In general, it is noted that interlayer post-processing through machining every 2 layers led to best results in terms of wall deformation.

3.1 QUANTITATIVE ANALYSIS OF DISTORTION

In order to analyse part deformation in each case, width in the cross direction (Figure 3) and height of samples were measured. In Table 4 values of those measurements are shown.

Sample	Width		Height
	Minimum	Maximum	
AM only – 0 dwell	1.97	3.76	13.51
AM only – 10 dwell	1.51	2.79	12.11
LR every 2 layers	1.68	3.18	14.96
LR every 5 layers	1.70	2.80	15.02
LR every 10 layers	1.62	2.9	-
Machining every 2 layers	1.83	1.90	14.5
Machining every 5 layers	1.69	3.23	13.78
Machining every 10 layers	1.56	3	14.37

Table 4. Width and height of samples built with different post-processing conditions.

Figure 4 shows the shape the variation of width and height with respect to the nominal value corresponding to each sample.

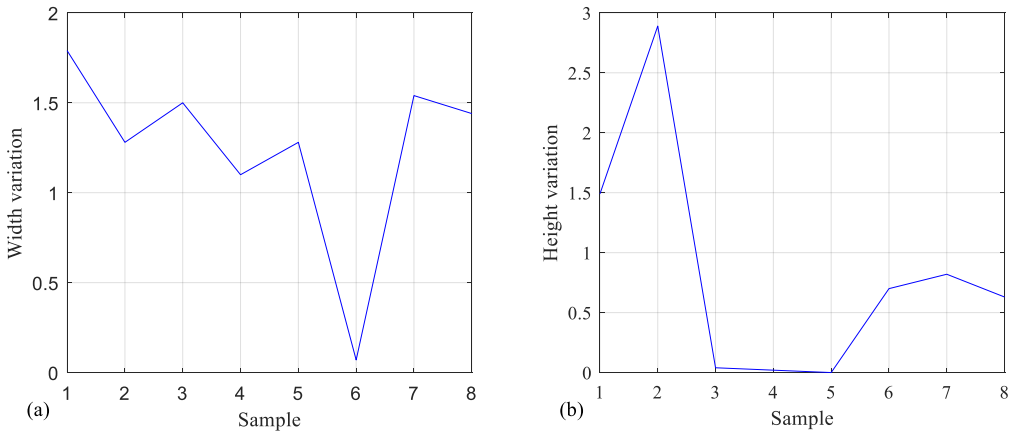

Figure 4. Shape variations in samples: (a) width variation in each sample and (b) height variation with respect to the nominal.

According to the width variation, as it was also noticeable in the cross-sections included in Figure 3, it is seen that sample 6 (post-processed through machining every 2 layers) showed the lowest width variation along the build direction. Sample no. 1, that corresponds to the wall generated without post-processing and with no dwell time showed the largest width variation. Regarding the height variation, highest variation with respect to the nominal value was measured for sample no.2 (AM only and 10s dwell time). Samples post-treated showed the lowest difference with respect to the theoretical value and those post-process through machining showed and improvement with respect to those as-printed.

In addition to the external appearance of the walls, a more detailed analysis of their porosity and mechanical properties has been conducted that will be introduced in the next sections. With this aim, samples were cut in the transversal direction so that the evolution of those parameters in the built direction could be analysed.

3.2 POROSITY OF DEPOSITED PARTS

In Table 5 porosity values corresponding to the different walls deposited are summarized. LR and M parameters in the table refer to laser remelting and machining post-processes conducted on the samples after the deposition of different amount of layers (2, 5 and 10), respectively.

Post-processing	AM 0 dwell	AM 10s dwell	LR 2	LR 5	LR 10	M 2	M 5	M 10
Porosity %	0.09	0.31	0.05	0.06	0.12	0.16	0.15	0.25

Table 5. Porosity values measured in the cross-section of samples under different post-processing conditions.

From the porosity values summarized in the table, it can be extracted that LR post-processing led to the samples with highest density. It was noted that both post-processes improved the density of generated components when compared to the as-deposited samples. Additionally, it is seen that by applying the post-process after few deposition layers leads to better porosity results.

3.3 EVOLUTION OF HARDNESS IN THE BUILD DIRECTION

Figure 5 shows the evolution of hardness measured at different distances from the top of the deposited samples.

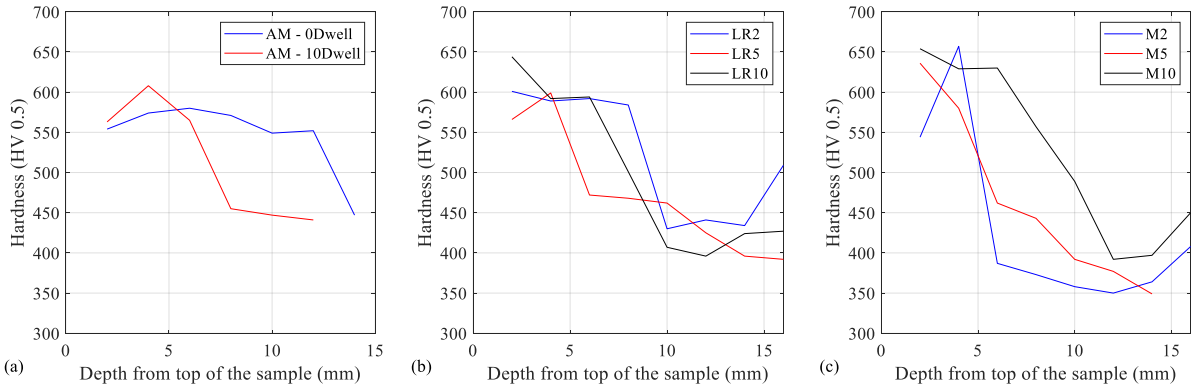

Figure 5. Hardness values measured in the samples: (a) as deposited, (b) after LR post-processing and (c) after machining post-processing.

It is observed that hardness values increase along the build direction regardless of the post-processing method employed and also for the as-deposited samples. In comparing the three cases, it is seen that highest hardness values were measured for the machined samples. Concretely, post-processing through machining after the deposition of 10 layers led to the highest hardness values among all tests.

Figure 5 (a) shows that introducing a dwell time between depositions of layers does not improve the hardness generated. Through the analysis of Figure 5 (b) no clear correlation can be extracted between hardness values and number of layers deposited previous to the post-processing. Finally, in Figure 5 (c), it can be noted that when using machining as post-processing, hardness values decrease with the decrease on the number of layers deposited before the post-processing is applied.

4. DISCUSSION

Once the main results obtained in the experimental tests have been introduced, in this section a discussion of these results is presented along with a deep analysis of the influence of process parameters on process behaviour.

In comparing the samples generated by using only AM and with different dwell times, it is observed that deformation of the sample with no dwell time is higher, as it is also the hardness and the temperature reached on the deposition area. This can all be related to a higher heat accumulated along the layers as consequence of the continuous application of laser on the sample. With no dwell time, there

is no time for the sample to reduce the temperature before a new LR track is applied, which leads to excessive melting and shape distortion. However, this effect benefits the resulting density and hardness that are higher in the sample generated with no dwell.

As mentioned above temperatures generated during deposition process were also measured and analysed in order to study their influence on the obtained walls characteristics. Figure 6 shows an example of a temperature colour map captured with the thermal camera during the deposition of one of the samples. In the figure, the studied area (named as Area 1 in the figure) is also remarked. As it is seen, the analysed temperature values focus only on the deposition area.

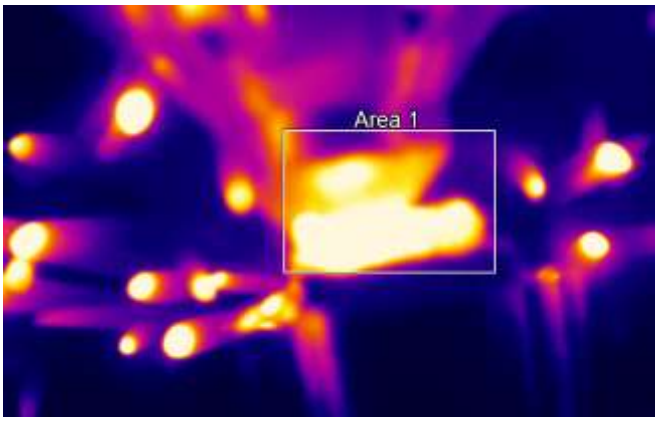

Figure 6. Temperature colour map measured with the thermal camera during one of the depositions.

Figure 7 shows the temperature values measured for both walls deposited with no post-processing relative to the chamber temperature once the laser was switched off. As the only aim of this analysis is to accomplish a comparative study of the effect of each deposition strategy, relative temperatures were taken as reference.

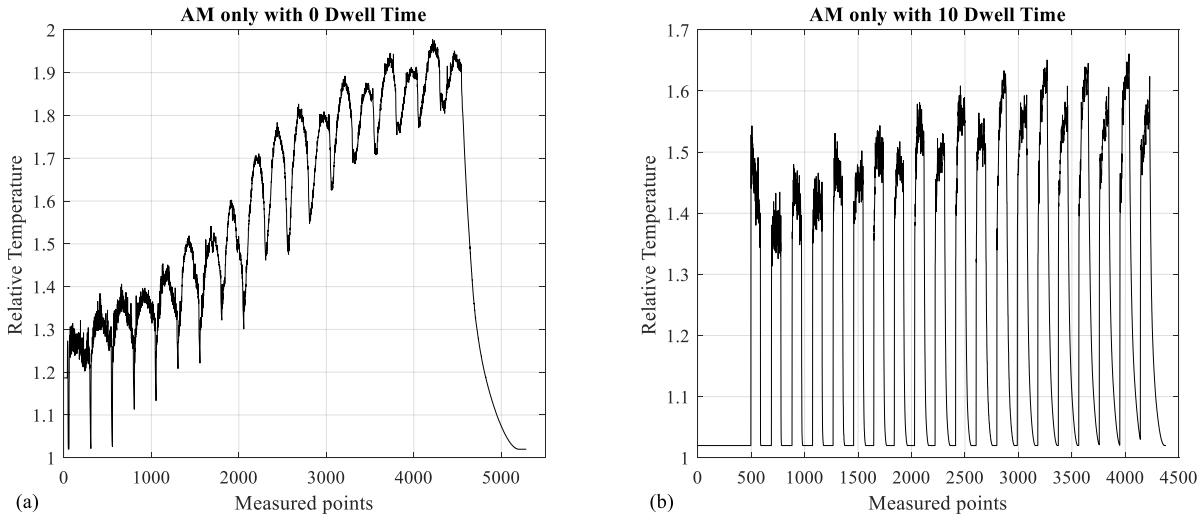

Figure 7. Temperature values measured during the deposition of H13 walls with no post-processing and (a) no dwell time and (b) 10s dwell time.

It can be seen in Figure 7 (a) that, when no dwell time is set between deposition tracks, wall temperature increases with the increase of the deposited layers with an almost linear trend. It is worth noting that, on this case, not only does the peak values increase, but the base temperature increases as well. Therefore it can be concluded that with this strategy, the substrate and previously deposited layers re-heated as consequence of the subsequent depositions. For the sample deposited with 10s dwell time between tracks Figure 7 (b) it was observed that during the first layers, dwell time was enough for the

substrate and the deposited bulk to cool down to the base temperature. However, after a certain layer was deposited, dwell time was not enough for temperature to return to the base temperature. This is a consequence of the increasing accumulation of heat. In comparing both strategies, it was observed that the maximum temperature reached with 10s dwell time strategy was remarkably lower that the one with no dwell time. As it was shown in Figure 3 (a) and (b), the sample created with 10s dwell time presented a better performance and less distortion, which can be related to the lower heat accumulated in this experiment.

As for distortion, samples generated with different layers deposited before LR do not show a significant difference. Similarly, no clear influence is observed for hardness evolution and temperatures measured. However, porosity is seen to increase with increasing number of layers before applying LR. This is due to the better melting conditions that are achieved when LR is applied more continuously. It is worth noting that in all these samples, a dwell time between laser paths was set that could help in sample cooling and lead to a better process performance. Temperatures arising in these samples are analysed next.

Figure 8 shows the relative temperature values measured during the deposition conducted with post-processing through laser remelting every two layers.

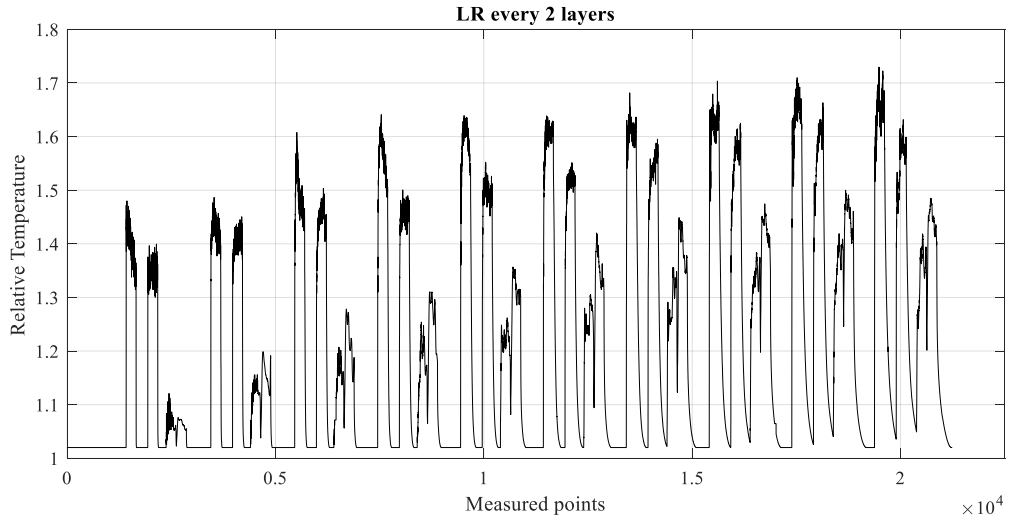

Figure 8. Temperature values measured during the deposition of H13 walls with post-processing through laser remelting every 2 layers.

It can be observed that for each couple of depositions, temperatures during the second layer are always slightly lower than those measured during the first deposition. As expected, temperatures during laser remelting tracks are lower than those generated during powder deposition due to the lower laser power values employed during remelting laser tracks. In addition, temperatures increase with the increase of deposited layers due to the heat accumulation in the bulk. Finally, as shown in the previous section, here it can be observed that during the first layers dwell time is enough for the material to cool down and recover the base temperature as well. However, with the increase of deposited layers and due to the mentioned hear accumulation, during the last depositions, temperatures reached higher values and the material cannot be cooled down to the base temperature during dwell time. Similar results were obtained for samples with laser remelting every 5 and every 10 layers (see Figure 9 and Figure 10).

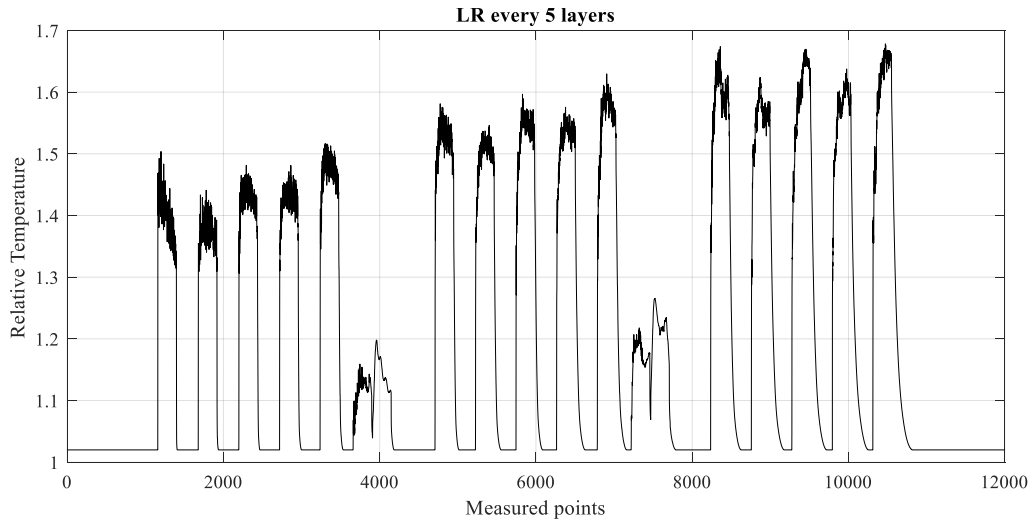

Figure 9. Temperature values measured during the deposition of H13 walls with post-processing through laser remelting every 5 layers.

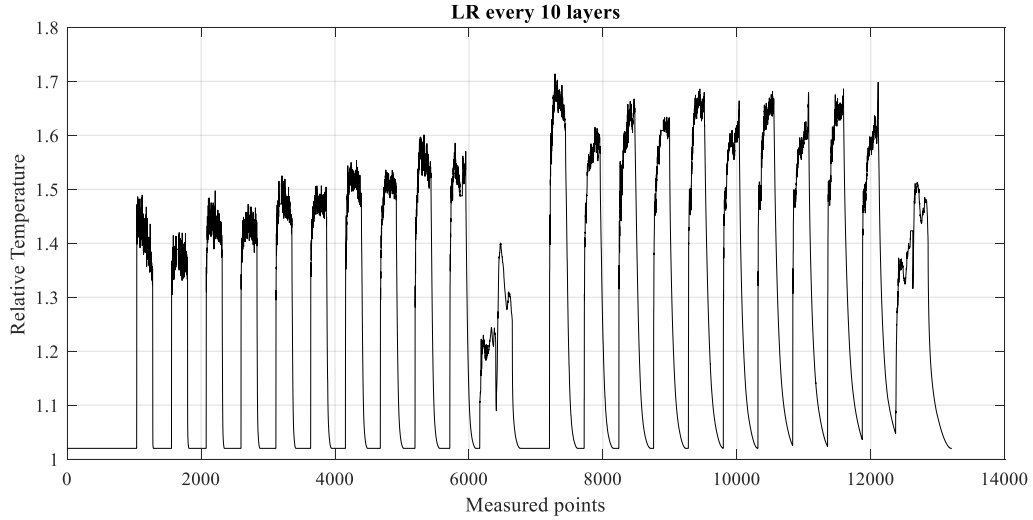

Figure 10. Temperature values measured during the deposition of H13 walls with post-processing through laser remelting every 10 layers.

Regarding the samples post-processed through face milling, it is observed that distortion of samples increases for increasing number of layers deposited before machining. This is due to the regenerative effect of the distortion that is relatively rectified each time a machining pass is conducted and the subsequent layers are deposited on a straight and fine surface. Concerning porosity values, no clear relation with machining was observed although the highest porosity value corresponds to the sample with the highest amount of layers deposited before machining. It is assumed, therefore, that also in the case of porosity, a more frequent machining post-processing will generate better results. Finally, hardness is seen to increase with increasing number of layers before machining. No temperature measurement was made during machining post-processing because the temperatures that arise during these operations are much lower than that generated by the laser. Heat generated during machining operations is evacuated through the chip removed from the part and along the surfaces of the cutting tool and it does not affect the workpiece in a significant way. Therefore, there is no point in comparing that parameter.

As a summary of the temperature results, Figure 11 shows the evolution of average relative temperatures measured along the layers deposited for the different post-processing techniques evaluated.

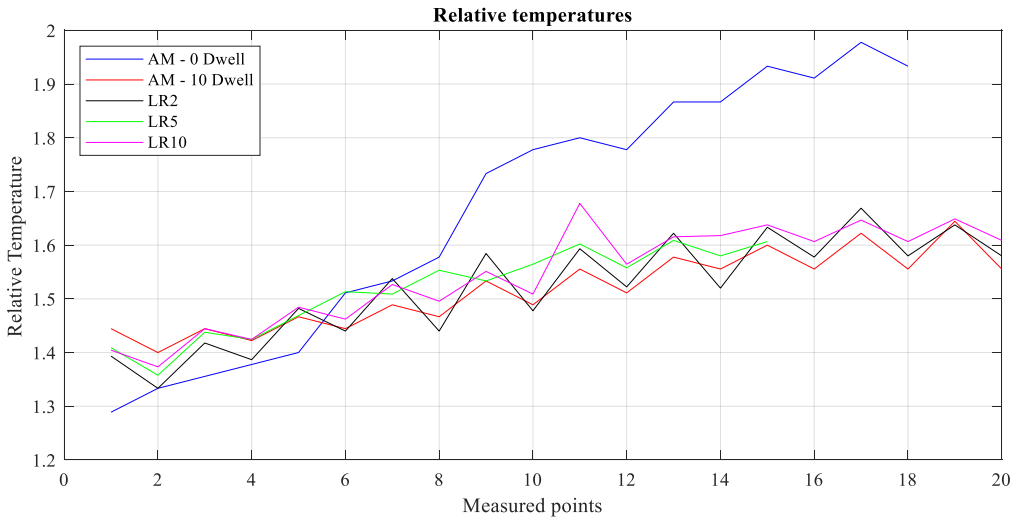

Figure 11. Comparison of average relative temperatures measured for each layer considering the different deposition strategies tested.

It can be observed that, among the different cases, additive manufacturing with no dwell time and no post-processing leads to the highest temperature values that increase sharply once the 8th layer is deposited. In comparing the values measured for the rest of cases, no remarkable difference in the evolution of relative temperature is noticed. According to the actual temperature values reached in each test, during the additive manufacturing with no dwell time test, a maximum temperature near 900ºC was registered. For the rest of cases, the maximum temperature did not exceed 750ºC.

5. CONCLUSIONS

This paper presents an experimental analysis of the hybrid additive manufacturing of H13 steel alloy. Additively manufactured samples have been subjected to post-processing through machining (face-milling) and laser re-melting to analyse the benefits provided by these treatments. The crack formation, porosity and microstructure of the generated samples were studied. Characteristics of as-deposited and treated samples have been compared to verify the benefits provided by hybrid additive manufacturing. Additionally, the number of layers deposited before post-processing is applied was also varied to study its effect on the obtained results. The following conclusions were extracted from this work:

- Regarding dimensional distortion of the samples, the wall post-treated with machining every two layers showed best results. It is noted that machining avoid the accumulation of distortions and enables the new layers to be deposited in a smooth surface.
- However, as for the porosity, post-processing through laser remelting led to best results.
- Finally, the hardness measurements revealed that samples post-treated had higher hardness values, but achieved hardness values were similar regardless the post-processing technique employed. Samples showed highest hardness values at the top layers.

Taking into account all the above, it has been shown in this paper that interlayer post-processing allows a significant improvement in the quality and properties of components manufactured by L-DED. Each technique improves different part properties and therefore, the applied post-processing technique should be selected depending on the desired properties of the parts.

6. REFERENCES

[1] S.T. Newman, Z. Zhu, V. Dhokia, A. Shokrani, Process planning for additive and subtractive manufacturing technologies, CIRP Ann. - Manuf. Technol. 64 (2015) 467–470. doi:10.1016/j.cirp.2015.04.109.

[2] 3dhubs, Producing Metal Parts - CNC vs. Additive Manufacturing, (n.d.).

[3] G. Manogharan, R. Wysk, O. Harrysson, R. Aman, AIMS - A Metal Additive-hybrid Manufacturing System: System Architecture and Attributes, Procedia Manuf. 1 (2015) 273–286. doi:10.1016/j.promfg.2015.09.021.

[4] D. Herzog, V. Seyda, E. Wycisk, C. Emmelmann, Additive manufacturing of metals, Acta Mater. 117 (2016) 371–392. doi:10.1016/j.actamat.2016.07.019.

[5] A. Azarniya, X.G. Colera, M.J. Mirzaali, S. Sovizi, F. Bartolomeu, M. k. St Weglowski, W.W. Wits, C.Y. Yap, J. Ahn, G. Miranda, F.S. Silva, H.R. Madaah Hosseini, S. Ramakrishna, A.A. Zadpoor, Additive manufacturing of Ti–6Al–4V parts through laser metal deposition (LMD): Process, microstructure, and mechanical properties, J. Alloys Compd. 804 (2019) 163–191. doi:10.1016/j.jallcom.2019.04.255.

[6] J.O. Milewski, Corrosion News, 2018. doi:10.1002/maco.201870124.

[7] A. Jiménez, P. Bidare, H. Hassanin, F. Tarlochan, S. Dimov, K. Essa, Powder-based laser hybrid additive manufacturing of metals : a review, Int. J. Adv. Manuf. Technol. (2021). doi:https://doi.org/10.1007/s00170-021-06855-4.

[8] E.P.M. Association, Introduction To Additive Manufacturing Technology, (2017) 1–56.

[9] N.N. Kumbhar, A. V. Mulay, Post Processing Methods used to Improve Surface Finish of Products which are Manufactured by Additive Manufacturing Technologies: A Review, J. Inst. Eng. Ser. C. 99 (2018) 481–487. doi:10.1007/s40032-016-0340-z.

[10] W.M. Tucho, P. Cuvillier, A. Sjolyst-Kverneland, V. Hansen, Microstructure and hardness studies of Inconel 718 manufactured by selective laser melting before and after solution heat treatment, Mater. Sci. Eng. A. 689 (2017) 220–232. doi:10.1016/j.msea.2017.02.062.

[11] D. Deng, R.L. Peng, H. Brodin, J. Moverare, Microstructure and mechanical properties of Inconel 718 produced by selective laser melting: Sample orientation dependence and effects of post heat treatments, Mater. Sci. Eng. A. 713 (2018) 294–306. doi:10.1016/j.msea.2017.12.043.

[12] V.A. Popovich, E. V. Borisov, A.A. Popovich, V.S. Sufiiarov, D. V. Masaylo, L. Alzina, Impact of heat treatment on mechanical behaviour of Inconel 718 processed with tailored microstructure by selective laser melting, Mater. Des. 131 (2017) 12–22. doi:10.1016/j.matdes.2017.05.065.

[13] H. Hassanin, K. Essa, C. Qiu, A.M. Abdelhafeez, N.J.E. Adkins, M.M. Attallah, Net-shape manufacturing using hybrid selective laser melting/hot isostatic pressing, Rapid Prototyp. J. 23 (2017) 720–726. doi:10.1108/RPJ-02-2016-0019.

[14] S. Huang, W.Y. Yeong, Laser re-scanning strategy in selective laser melting for part quality enhancement: A review, Proc. Int. Conf. Prog. Addit. Manuf. 2018–May (2018) 413–419. doi:10.25341/D4GP4J.

[15] E. Yasa, J. Deckers, J.P. Kruth, The investigation of the influence of laser re-melting on density, surface quality and microstructure of selective laser melting parts, Rapid Prototyp. J. 17 (2011) 312–327. doi:10.1108/13552541111156450.

[16] W. Yu, S.L. Sing, C.K. Chua, X. Tian, Influence of re-melting on surface roughness and porosity of AlSi10Mg parts fabricated by selective laser melting, J. Alloys Compd. 792 (2019) 574–581. doi:10.1016/j.jallcom.2019.04.017.

[17] X. Yang, J. Liu, X. Cui, G. Jin, Z. Liu, Y. Chen, X. Feng, Effect of remelting on microstructure and magnetic properties of Fe-Co-based alloys produced by laser additive manufacturing, J. Phys. Chem. Solids. 130 (2019) 210–216. doi:10.1016/j.jpcs.2019.03.001.

[18] K. Wei, M. Lv, X. Zeng, Z. Xiao, G. Huang, M. Liu, J. Deng, Effect of laser remelting on deposition quality, residual stress, microstructure, and mechanical property of selective laser melting processed Ti-5Al-2.5Sn alloy, Mater. Charact. 150 (2019) 67–77. doi:10.1016/j.matchar.2019.02.010.

[19] AZoM, H13 Tool Steel - Chromium Hot-Work Steels, (2013). https://www.azom.com/article.aspx?ArticleID=9107 (accessed March 9, 2020).

[20] R. Cottam, J. Wang, V. Luzin, Characterization of microstructure and residual stress in a 3D H13 tool steel component produced by additive manufacturing, J. Mater. Res. 29 (2014) 1978–1986. doi:10.1557/jmr.2014.190.

[21] U. Articek, M. Milfelner, I. Anzel, Synthesis of functionally graded material H13/Cu by LENS technology, Adv. Prod. Eng. Manag. 8 (2013) 169–176. doi:10.14743/apem2013.3.164.

[22] G. Telasang, J. Dutta Majumdar, G. Padmanabham, M. Tak, I. Manna, Effect of laser parameters on microstructure and hardness of laser clad and tempered AISI H13 tool steel, Surf. Coatings Technol. 258 (2014) 1108–1118. doi:10.1016/j.surfcoat.2014.07.023.

[23] J.S. Park, J.H. Park, M.G. Lee, J.H. Sung, K.J. Cha, D.H. Kim, Effect of Energy Input on the Characteristic of AISI H13 and D2 Tool Steels Deposited by a Directed Energy Deposition Process, Metall. Mater. Trans. A Phys. Metall. Mater. Sci. 47 (2016) 2529–2535. doi:10.1007/s11661-016-3427-5.

[24] J. Choe, J. Yun, I.M.D.O.O. Jung, D. Yang, S. Yang, Y. Kim, J. Yu, Densifying Method in Additive Manufacturing Process of H13 Tool Steel: Laser re-melting, (2018) 232–236.

[25] G. Payne, A. Ahmad, S. Fitzpatrick, P. Xirouchakis, W. Ion, M. Wilson, Remanufacturing H13 steel moulds and dies using laser metal deposition, Adv. Transdiscipl. Eng. 3 (2016) 93–98. doi:10.3233/978-1-61499-668-2-93.

[26] M.-H. Multi-tasking, INTEGREX i-400S AM, (n.d.). https://www.mazakusa.com/machines/integrex-i-400s-am/ (accessed February 4, 2020).

[27] Additive Manufacturing Solutions, n.d.